NUMERICAL CALCULATION OF A THREE-DIMENSIONAL LAMINAR COMPRESSIBLE BOUNDARY LAYER ON PROFILED TRIANGULAR WINGS WITH SUPERSONIC FRONT EDGES

V. N. Vetlutskii and T. V. Poplavskaya

UDC 532.526

In the investigation of the aerodynamics of wings, analysis of the coefficients of friction and heat exchange on the surface of a body is of great significance; these coefficients are determined from calculation of the boundary layer on the wing. At the present time there are a number of publications on the numerical calculation of an automodel compressible layer on conical bodies [1-3]. The calculation of a three-dimensional laminar boundary layer on the sharpened body of a bielliptical cross section is realized in [4]. In [5] the calculation of a three-dimensional boundary layer in the laminar and turbulent modes of flow on a plane triangular wing is carried out.

The present article describes the formulation of the problem and an algorithm for calculating a three-dimensional compressible laminar boundary layer on a profiled wing with supersonic front edges. The results of its realization for the windward and leeward sides of the wing with an angle of sagitallity of $\chi = 45°$ at a Mach number of $M_\infty = 3$ and for the windward side of the wing with the same χ for $M_\infty = 3$ and 6 for a series of angles of incidence α are presented. The influence of the Mach number, the angle of incidence, and the relative thickness of the profile on the coefficient of friction is investigated.

1. The surface of the wing is assumed to be smooth and its equation of the form $y = F(x, z)$ is given in the Cartesian system of coordinates (x, y, z) with its origin at the tip of the wing (Fig. 1). The $z = 0$ plane coincides with the vertical plane of symmetry. The front and rear edges of the wing lie in the $y = 0$ plane. The velocity vector of the oncoming flow U_∞ lies in the vertical plane of symmetry of the streamlined body and constitutes the angle of incidence α with the x axis.

To describe the boundary layer, a nonorthogonal coordinate system (ξ, η, ζ), associated with the surface of the body, is introduced:

$$\xi = x, \quad \zeta = 1 - z/f(x).$$

Here the coordinate ζ is read from the front edge; η is the normal to the surface; and $z = f(x)$ is the equation of the front edge. All of the parameters are rendered dimensionless with regard to the length of the central chord L and the values of the same parameters in the oncoming flow (index ∞), with the exception of

$$\bar{\eta} = \eta\sqrt{\mathrm{Re}_L}/L, \quad \bar{v} = v\sqrt{\mathrm{Re}_L}/L, \quad \bar{p} = p/\rho_\infty U_\infty^2,$$
$$\mathrm{Re}_L = \rho_\infty U_\infty L/\mu_\infty, \quad \mathrm{Pr} = \mu_\infty c_{p\infty}/k_\infty, \quad M_\infty = U_\infty/\sqrt{\gamma RT_\infty}$$

(the lines are omitted in the equations below). In accordance with [6], the matrix $B = \|\beta_j^{i'}\|$, of the components of the covariant basis vectors corresponding to the axes ξ, η, ζ ($i', j = 1, 2, 3$), and the metrical coefficients g_{11}, g_{12}, g_{22}, g, are written out [7].

In order to eliminate the singularity at the front edge and decrease the dependence of the external of the boundary layer on the longitudinal coordinate, a new variable $\lambda = \eta/\sqrt{\xi\zeta}$. Then the equations of the boundary layer in physical variables [8] have the form

$$\xi\zeta\left[\frac{\partial}{\partial\xi}(\rho u\sqrt{g/g_{11}}) + \frac{\partial}{\partial\zeta}(\rho w\sqrt{g/g_{22}})\right] + \sqrt{g}\frac{\partial J}{\partial\lambda} + \xi\rho w\sqrt{g/g_{22}}/2 + \zeta\rho u\sqrt{g/g_{11}}/2 = 0. \qquad (1.1)$$

Novosibirsk. Translated from Prikladnaya Mekhanika i Tekhnicheskaya Fizika, No. 5, pp. 88-94, September-October, 1993. Original article submitted February 3, 1992; revision submitted October 1, 1992.

0021-8944/93/3405-0677$12.50

TABLE 1

Wing	α, deg	M_∞		
		3		6
		$c_{\mathcal{L}}$ (CF_x^*)	c_W (CF_x^*)	c_W (CF_x^*)
F	0	0,05 (2,038)	0,05 (2,038)	—
	5	0,05 (1,784)	0,04 (2,224)	—
	8	0,05 (1,630)	0,03 (2,291)	—
G	0	—	0,03 (1,990)	0,03 (1,910)
	5	—	0,03 (2,222)	0,03 (2,521)
	10	—	—	0,03 (3,128)

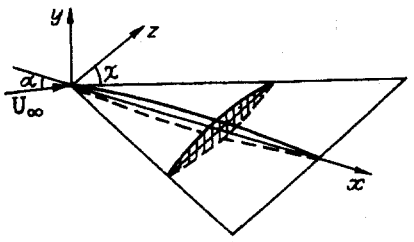

Fig. 1

We will write the equations of motion and energy with an identical structure as

$$a_i \frac{\partial f_i}{\partial \xi} + b_i \frac{\partial f_i}{\partial \zeta} + c_i \frac{\partial f_i}{\partial \lambda} - \frac{\partial}{\partial \lambda}\left(d_i \frac{\partial f_i}{\partial \lambda}\right) + e_i = 0 \quad (i = 1, 2, 3), \tag{1.2}$$

where

1) $f_1 = u$, $a_1 = \xi\zeta\rho u/\sqrt{g_{11}}$, $b_1 = \xi\zeta\rho w/\sqrt{g_{22}}$, $c_1 = J$, $d_1 = \mu$, $e_1 = \xi\zeta\,(A_6 - A_4)$;

2) $f_2 = w$, $a_2 = \xi\zeta\rho u/\sqrt{g_{11}}$, $b_2 = \xi\zeta\rho w/\sqrt{g_{22}}$, $c_2 = J$, $d_2 = \mu$, $e_2 = \xi\zeta\,(B_6 - B_4)$;

3) $f_3 = T$, $a_3 = c_p\xi\zeta\rho u/\sqrt{g_{11}}$, $b_3 = c_p\xi\zeta\rho w/\sqrt{g_{22}}$, $c_3 = c_p J$, $d_3 = k/\mathrm{Pr}$,

$$e_3 = \xi\zeta\,(A_5 u + B_5 w) - \mathrm{M}_\infty^2\,(\gamma - 1)\,\mu\left[\left(\frac{\partial u}{\partial \lambda}\right)^2 + \left(\frac{\partial w}{\partial \lambda}\right)^2 + 2\cos\varphi\,\frac{\partial u}{\partial \lambda}\frac{\partial w}{\partial \lambda}\right].$$

The system of equations (1.1), (1.2) is closed by the equation of state

$$\rho = \gamma \mathrm{M}_\infty^2 p/T.$$

Here, instead of the velocity component v, the mass flow is introduced:

$$J = \rho\left(\sqrt{\xi}\,v - \frac{\eta}{2\sqrt{\xi g_{11}}}\,u\right)\sqrt{\zeta} - \frac{\eta\sqrt{\xi}}{2\sqrt{\zeta g_{22}}}\,\rho w;$$

where φ is the angle between the axes of the coordinates ξ, ζ; $\cos\varphi = g_{12}/\sqrt{g_{11}g_{22}}$; A_1, A_2, A_3, B_1, B_2, B_3 are taken in the same form as in [8].

The system of equations (1.1), (1.2) is solved in the region Ω ($\xi \geq \xi_0$, $0 \leq \zeta \leq \zeta_k$, $0 \leq \lambda \leq \lambda_e(\xi, \zeta)$) for the following boundary conditions:

TABLE 2

M_∞	c_w	α, deg					
		0			5		
		cF_x	cX_0	$\frac{cF_x}{cX_0}$, %	cF_x	cX_0	$\frac{cF_x}{cX_0}$, %
3	0	0,0053	0,0053	100	0,0061	0,0261	23
	0,03	0,0062	0,0093	67	0,0070	0,0325	21,5
6	0	0,0050	0,0050	100	0,0068	0,0137	49,5
	0,03	0,0060	0,0076	79	0,0080	0,0190	43

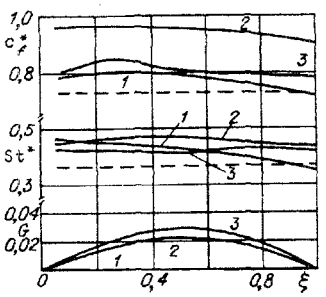

Fig. 2

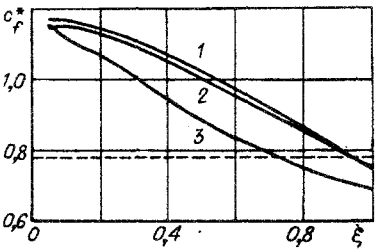

Fig. 3

$$\xi = \xi_0: \quad u = u_0(\zeta, \lambda), \quad w = w_0(\zeta, \lambda), \quad T = T_0(\zeta, \lambda);$$
$$\zeta = 0: \quad u = u_\delta(\xi, \lambda), \quad w = w_\delta(\xi, \lambda), \quad T = T_\delta(\xi, \lambda);$$
$$\lambda = 0: \quad u = w = J = 0, \quad T = T_w;$$
$$\lambda = \lambda_e(\xi, \zeta): \quad u = u_e(\xi, \zeta), \quad w = w_e(\xi, \zeta), \quad T = T_e(\xi, \zeta), \quad p = p_e(\xi, \zeta).$$

The index e corresponds to the values of the parameters at the external bounary of the boundary layer and w to the values at the surface of the wing. The cross section $\xi = \xi_0$ is fixed at the conical tip of the body, and the profiles u_0, w_0, T_0 are taken from the automodel solution for the tip. At the front edge $\zeta = 0$, the profiles u_δ, w_δ, T_δ are determined from the solution of the ordinary differential equations obtained from (1.1), (1.2) for $\zeta \to 0$ under the assumption of the boundedness of all of the functions being sought and their derivatives [7]. At the surface of the body ($\lambda = 0$) the adhesion conditions that are usual for a viscous liquid and the equality of the temperatures of the gas and the wall are assumed. At the external boundary ($\lambda = \lambda_e(\xi, \zeta)$ the parameters of the boundary layer are taken from the calculations of a nonviscous gas flowing around the wing [9, 10] and are interpolated with a smoothing cubic spline, as is the equation of the wing surface.

To increase the calculation accuracy with a uniform differential grid, new independent variables (t, s, n) are introduced, with the aid of which the regions of large gradients of the functions being sought can be expanded. For this the substitution

$$\xi = t, \quad \zeta = \zeta(s), \quad \lambda = \lambda(t, s, n),$$

is performed, where $\zeta(s)$ is taken in the form of a third-degree polynomial compressing the nodes of the differential grid at the plane of symmetry of the wing. The conversion $\lambda(t, s, n)$ is set such that in the region of large gradients of the functions in the λ direction the spacing of the differential grid in physical variables is small [7].

2. To begin with, by means of the Marsh method in the s coordinate the automodel boundary layer in the conical section was calculated; for this a purely implicit scheme was used. The resulting values of the gas dynamic parameters u_0, w_0, T_0 were used as the initial conditions in the $t = t_0$ cross section in the conical section. Then the Marsh method was used in the t coordinate to solve the three-dimensional equations of the boundary layer. A two-layer implicit weighted differential scheme, absolutely stable at the values of the weighting factor $0.5 \leq \theta \leq 1.0$, like the one described in detail in [11], was used.

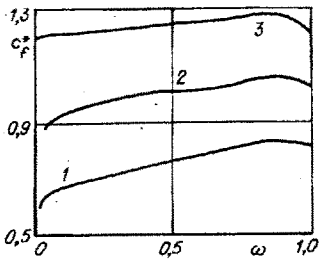

Fig. 4

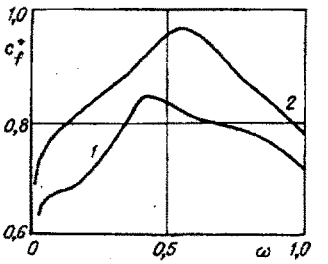

Fig. 5

In accordance with the resulting velocity and temperature profiles in each cross section, the components of the coefficients of friction pressure and the Stanton number on the surface of the body were calculated:

$$c_{f1}^* = c_{f1}\sqrt{\mathrm{Re}_\xi\,\zeta} = \frac{\tau_\xi}{0{,}5\rho_\infty U_\infty^2}\sqrt{\mathrm{Re}_\xi\,\zeta},$$

$$c_{f2}^* = c_{f2}\sqrt{\mathrm{Re}_\xi\,\zeta} = \frac{\tau_\zeta}{0{,}5\rho_\infty U_\infty^2}\sqrt{\mathrm{Re}_\xi\,\zeta},$$

$$c_f^* = \sqrt{c_{f1}^{*2} + c_{f2}^{*2} + 2c_{f1}^* c_{f2}^* \cos\varphi}, \quad \mathrm{St}^* = \mathrm{St}\sqrt{\mathrm{Re}_\xi\,\zeta} = \frac{q}{\rho_\infty U_\infty (h_\infty - h_w)}\sqrt{\mathrm{Re}_\xi\,\zeta}.$$

Here Re_ξ is the Reynolds number calculated from the parameters of the incident flow and the distance ξ from the tip of the body; τ_ξ, τ_ζ are the components of the friction pressure; q is the heat flow at the surface of the wing; and h is the total enthalpy.

Also taken into account was the total contribution of the force of friction at the surface of the wing to the coefficients of the aerodynamic longitudinal and normal forces, which are determined from the formulas

$$CF_x^* = CF_x\sqrt{\mathrm{Re}_L} = \frac{X_T\sqrt{\mathrm{Re}_L}}{(1/2)\rho_\infty U_\infty^2 S} = 2\int_0^1\int_0^1 \frac{c_{f1}^*\cos\gamma\cos\vartheta}{\sqrt{\zeta}}\sqrt{\xi}\,d\xi d\zeta,$$

$$CF_y^* = CF_y\sqrt{\mathrm{Re}_L} = \frac{Y_T\sqrt{\mathrm{Re}_L}}{(1/2)\rho_\infty U_\infty^2 S} = 2\int_0^1\int_0^1 \frac{c_{f1}^*\sin\gamma\cos\vartheta + c_{f2}^*\sin\vartheta}{\sqrt{\zeta}}\sqrt{\xi}\,d\xi d\zeta,$$

where X_T, Y_T is the total force of friction in the longitudinal and nomral directions; λ is the angle between the vector c_{f1} and the ξ axis in a projection onto the (ξ, λ) plane; ϑ is the angle between the c_{f1} vector and the ξ axis in a projection onto the (ξ, ζ) plane; and S is the area of the surface of the wing. Computation of the integrals was carried out according to the trapezoid formula. An exception is the vicinity of the front edge, where the values of the integrals were determined analytically.

The overall resistance of the wing CX_0 was found from the formula

$$CX_0 = C_x + CF_x$$

where C_X is the wave resistance taken from the calculations of nonviscous flow around the wing and CF_X is the coefficient of friction resistance converted to the velocity coordinate system for a given Re_L.

A more detailed formulation of the problem and an algorithm for solving three-dimensional boundary layer equations are described in [7].

3. The resulting program was first tested by comparing the results of the calculation with the basic results for a plane plate [3] and with the data given in [5]. The results of these comparisons are given in [7]. A laminar boundary layer was then calculated for one enthalpic factor $H_W = h_W/h_\infty = 0.57$ for two profiled wings with the same sagittal angle $\chi = 45°$ and with the surface equations given in [9, 10]

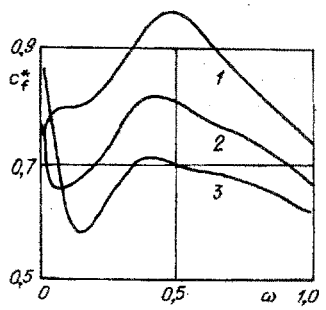

Fig. 6

$$F(\xi, \zeta) = 4c\,(1 - (1 - \zeta)^{1.5})\,(1 - \xi)\,\xi^{1.0526},$$
$$G(\xi, \zeta) = 4c\,(1 - (1 - \zeta)^{2})\,(1 - \xi)\,\xi^{1.047},$$

where c is the relative thickness of the windward surface c_w and of the leeward surface c_ℓ. All of the variants considered are given in Table 1.

Figure 2 shows the distribution of the parameters c_f^* and St* at the windward surface of wing G for $c_w = 0.03$, $M_\infty = 3$, $\alpha = 5°$ in cross sections $\zeta = 0$; 0.52; 0.85 (curves 1-3). Here the contour of the wing surface in these cross sections is represented. For comparison the dotted lines show the values of c_f^* and St* for the same defining parameters for a plane plate in the $\zeta = 0.52$ cross section. It is clear that the corrected parameters on the profiled wing increase their values for a plane plate by 30%. This is explained by the fact that the local angle of incidence of the tip section of the wing is approximately 5% higher than on the plate. An analogous situation also occurs with other angles of incidence.

For $M_\infty = 6$ the distribution of the coefficient of friction c_f^* on the windward surface of the same wing and with the same other defining parameters is given in Fig. 3. Here the numbering of the curves is the same as in Fig. 2. For $M_\infty = 6$ the value of c_f^* at the tip exceeds its value on the plane plate more significantly than for $M_\infty = 3$. Later, however, it begins to drop due to the more intensive increase in the thickness of the boundary layer.

The calculations for $M_\infty = 6$ and $\alpha = 0$-10° showed that the character of the behavior of the c_f^* and St* curves on the windward side is preserved. Only their absolute value varies by approximately 25% for an increase in α by 5°. This is illustrated in Fig. 4, in which for $\alpha = 0$, 5, 10° (lines 1-3) the distribution of the c_f^* parameter is represented as a function of the transverse coordinate $\omega = 1 - \zeta$ ($\omega = 1$ corresponds to the front edge) in the cross section $\xi = 0.5$ of wing G. An analogous comparison of the distribution of the c_f^* parameter on the windward side of wing G in the $\xi = 0.5$ cross section for $M_\infty = 3$ is performed in Fig. 5 (curves 1 and 2 correspond to $\alpha = 0$, 5°). Unlike $M_\infty = 6$, both curves are nonmonotonic.

The effect of the angle of incidence on the distribution of the coefficient of friction c_f^* on the leeward side of profiled wing F in the $\xi = 0.5$ cross section is shown in Fig. 6. The calculations were performed for $c_\ell = 0.05$, $M_\infty = 3$ and $\alpha = 0$, 5, 8° (curves 1-3). The character of the curves varies weakly with increase in α (with the exception of the region of the plane of symmetry in which the singular point of the nonviscous flow is located). Here the value of c_f^* decreases by ~15% with increase in α by 5°. Thus, it follows from Figs. 4-6 that for identical profile thicknesses and Mach numbers, the c_f^* (and also the St* curves) are qualitatively similar to one another at different angles of incidence.

In Table 1 under the values of the relative thickness of the windward c_w annd leeward c_ℓ surfaces of the wing the values of the total automodel coefficient of friction $CF_x^* = CF_x\sqrt{Re_L}$ for the surface in question are given; this coefficient increases practically linearly with increase in the angle of incidence for the windward side and decreases for the leeward side. The speed of increase for $M_\infty = 6$ is almost twice as great as for $M_\infty = 3$.

The contribution of the total friction pressure CF_x to the total resistance CX_0 for each surface of the wing was evaluated for $Re_L = 10^5$ (the Reynolds number was computed from the parameters of the oncoming flow and the length of the central chord). Table 2 presents the indicated quantities for the windward side of wing G for $c_w = 0.03$, $M_\infty = 3$ and 6, $\alpha = 0$

and 5°. For comparison their values for a plane triangular plate are given here for the same defining parameters [3]. It is evident that as M_∞ increases the value of CF_x for $\alpha = 0$ decreases somewhat, and for $\alpha = 5°$ it increases. However, the wave resistance drops significantly, which leads to an increase in the contribution of friction forces from 67% to 79% for $\alpha = 0$ and from 21.5% to 43% for $\alpha = 5°$.

From the data given in Table 2 it is possible to evaluate the effect of the relative thickness of the wing on the characteristics of the boundary layer. The value of CF_x for a profiled wing increases on the average by 15% in comparison with a triangular plate. However, in this case the wave resistance increases significantly, which leads to a decrease in the contribution of friction forces to the total resistance in comparison with a plane triangular plate. An analogous phenomenon is observed when the angle of incidence increases. Although the value of CF_x increases with increase of α from 0 to 5°, the wave resistance increases more significantly, and therefore the contribution of friction forces drops from 67% to 21.5% for $M_\infty = 3$ and from 79% to 43% for $M_\infty = 6$.

The contribution of friction forces for $M_\infty = 3$ to the total resistance of a wing whose windward side is formed by the surface G ($c_w = 0.03$), and whose leeward side is formed by surface F ($c_\ell = 0.05$) was evaluated. The evaluation was performed for $H_w = 0.57$ and $Re_L = 10^5$. The result was that with increase of α from 0 to 5°. The total resistance CF_x is practically invariant (0.0126 and 0.0125) while the total resistance CX_0 increases significantly (0.0225 and 0.0527) due to the wave resistance, which leads to a drop in the contribution of friction forces from 56% to 24%.

We note that the coefficient of friction resistance CF_x for the variants considered can easily be recalculated for any Reynolds number by dividing CF_x^* by $\sqrt{Re_L}$. The effect of the enthalpic factor on the parameters of the boundary layer has been studied using the model of a plane triangular plate [3].

LITERATURE CITED

1. V. A. Bashkin, "A laminar boundary layer in a compressible gas in a conical external flow," Proceedings of the Zhukovskii Central Aerohydrodynamic Institute, No. 1093 (1968).
2. V. N. Vetlutskii and V. L. Ganimedov, "A numerical solution of the problem of the boundary layer on an elliptical cone," ChMMSS, 8, No. 5 (1977).
3. V. N. Vetlutskii and T. V. Poplavskaya, "A compressible laminar boundary layer on a plane triangular plate with an associated shock wave," PMTF, No. 5 (1985).
4. L. M. Vetlutskaya and V. N. Vetlutskii, "Calculating a compressible laminar boundary layer on a tapered body," ChMMSS, 17, No. 5 (1986).
5. G. A. Shchekin, "Numerical calculation of a three-dimensional boundary layer in the laminar and turbulent regions of flow on a wing at supersonic flight speeds," in: An Experimental and Theoretical Investigation of the Aerodynamics of the Elements of an Aircraft and Its Parts [in Russian], MAI, Moscow (1983).
6. E. Hirschel and V. Cordulla, Transverse Flow of a Compressible Liquid [Russian translation], Mir, Moscow (1987).
7. V. N. Vetlutskii and T. V. Poplavskaya, "Calculating a laminar compressible boundary layer on a triangular profiled wing with supersonic front edges," Modelir. Mekh., 3(20), No. 6 (1989).
8. Yu. D. Shevelev, Three-Dimensional Problems in the Theory of Laminary Boundary Layers [in Russian], Nauka, Moscow (1977).
9. G. P. Voskresenskii, A. S. Il'ina, and V. S. Tatarenchik, "Supersonic flow around wings," Preprint of the Institute of Applied Mathematics, Academy of Sciences of the USSR, No. 104, 76 (1976).
10. G. P. Voskresenskii, A. S. Il'ina, and V. S. Tatarenchik, "Supersonic flow around wings with an associated shock wave," Tr. TsAGI, No. 1590 (1974).
11. L. M. Vetlutskaya and V. N. Vetlutskii, "Calculating a three-dimensional noncompressible laminar boundary layer on a flat plate with an obstruction," ChMMSS, 11, No. 4 (1980).
12. V. N. Vetlutskii and T. V. Poplavskaya, "Calculating a laminar boundary layer on the leeward side of a triangular plate with supersonic front edges," PMTF, No. 1 (1989).